



HAL
open science

Green hybrid zeolite coatings for on-orbit molecular decontamination

Mathieu Diboune, Habiba Nouali, Michel Soulard, Joël Patarin, Guillaume Rioland, Delphine Faye, Jean Daou

► **To cite this version:**

Mathieu Diboune, Habiba Nouali, Michel Soulard, Joël Patarin, Guillaume Rioland, et al.. Green hybrid zeolite coatings for on-orbit molecular decontamination. *Microporous and Mesoporous Materials*, 2020, 307, pp.110478. 10.1016/j.micromeso.2020.110478 . hal-03412209

HAL Id: hal-03412209

<https://hal.science/hal-03412209v1>

Submitted on 22 Aug 2022

HAL is a multi-disciplinary open access archive for the deposit and dissemination of scientific research documents, whether they are published or not. The documents may come from teaching and research institutions in France or abroad, or from public or private research centers.

L'archive ouverte pluridisciplinaire **HAL**, est destinée au dépôt et à la diffusion de documents scientifiques de niveau recherche, publiés ou non, émanant des établissements d'enseignement et de recherche français ou étrangers, des laboratoires publics ou privés.



Distributed under a Creative Commons Attribution - NonCommercial 4.0 International License

Green hybrid zeolite coatings for on-orbit molecular decontamination

Mathieu Diboune ^{a, b, d}, Habiba Nouali ^{a, b}, Michel Soulard ^c, Joël Patarin ^c, Guillaume Rioland ^d, Delphine Faye ^d, T. Jean Daou ^{a, b, *}

^a Université de Haute-Alsace (UHA), Axe Matériaux à Porosité Contrôlée (MPC), Institut de Science des Matériaux de Mulhouse (IS2M), 3b rue Alfred Werner, F-68093 Mulhouse, France

^b Université de Strasbourg, Strasbourg, France

^c Zéphir Alsace, 15 rue des Frères Lumière, F-68350 Brunstatt-Didenheim, France

^d Centre National d'Etudes Spatiales (CNES), Service Laboratoires & Expertise, 18 avenue Edouard Belin, F-31401 Toulouse Cedex 9, France

* Corresponding author. Tel.: + 33 3 89 33 67 39

E-mail address: jean.daou@uha.fr (T. J. Daou)

KEYWORDS

Hybrid zeolite coatings
Molecular decontamination
Organic-inorganic binders
Adhesion properties
Adsorption capacities

Abstract

FAU-type and MFI-type green hybrid zeolite coatings were developed for on-orbit molecular decontamination application by using a mixture of an organic binder (silicone resin) and an inorganic binder (suspension of colloidal silica nanoparticles). The zeolite content in the final dry coatings varies from 80 to 85 wt. % whereas the total amount of binders varies from 15 to 20 wt. %. This amount of binder was sufficient to give the zeolite coating interesting adhesion and cohesion properties. In fact, by using an equal amount of each binder, homogeneous films without significant cracks were obtained on an aluminum alloy substrate which is the main constituent of satellites. Nitrogen adsorption-desorption measurements revealed almost no loss of micropore volume of zeolite coatings. Adsorption experiments of an organic pollutant were carried out using *n*-hexane as probe molecule. The *n*-hexane adsorption capacities of FAU-type hybrid zeolite coatings (136 to 143 mg/g_{anhydrous zeolite}) are lower than that of pure FAU-type zeolite (180 mg/g_{anhydrous zeolite}) due to water co-adsorption. The *n*-hexane adsorption capacities of MFI-type zeolite coatings (103 to 106 mg/g_{anhydrous zeolite}) are similar to that of pure MFI-type zeolite (110 mg/g_{anhydrous zeolite}).

1. Introduction

One of the major issues in the space industry is the on-orbit molecular contamination. The harmful effects of this contamination of on-board equipment such as thermal control surfaces, electronic and optical devices, and detectors are now well known [1-3]. Indeed, once satellites are in orbit, the temperature can vary typically from -110 °C to 150 °C under high vacuum [4], this phenomenon induces an outgassing of organic pollutants emitted from the spacecraft materials. This contamination is impossible to control once satellites are launched and deposition of those molecules may occur on the surface of the above-mentioned equipment depending on the thermal environment. In order to better understand what is happening during the molecular contamination process, several studies have been carried out by the National Aeronautics and Space Administration (NASA) and the French Space Agency (CNES) to determine the chemical nature of these organic pollutants. It appears that molecules such as plasticizers, silicones and hydrocarbons are mainly responsible for this contamination [1, 4, 5]. In order to limit this phenomenon, several molecular adsorbents such as activated charcoal, mesoporous silica and zeolites have been tested for the capture and retention of these pollutants in orbit. Thanks to their adsorption capacities and, moreover, their ability to trap organic pollutants at a very low concentration at low pressure [6], zeolites appeared to be the most effective candidates to mitigate this contamination issue [7]. By using different shapings, these molecular adsorbents have been successfully used by CNES to trap organic pollutants in sensitive flight hardware [2-5, 8, 9].

Zeolites belong to the class of microporous solids. Their frameworks are a sequence of TO₄ tetrahedral units where T generally represents either a silicon or an aluminum atom. This TO₄ tetrahedra assembly defines a system of regular channels or cavities of molecular dimensions which has the ability to communicate with the external environment. Due to their pore size, high thermal stability and also their Brønsted acid properties, zeolites are widely used for adsorption and catalysis applications [10-15].

To date, almost 250 different structural types of zeolites have been approved by the Structural Commission of the International Zeolite Association (IZA) but only a small part of them is used on an industrial scale [16].

The synthesis of zeolites generally leads to the formation of fine crystallized powder which can be a source of particulate contamination. That is why zeolites have to be shaped to avoid this type of contamination in satellites. Prior to their industrial applications, zeolites can be shaped into tablets, pellets, beads and extrudates by the addition of organic or inorganic binders such as alumina [17], Portland cement [18, 19], clays [20, 21] and poly(vinyl alcohol) [22]. These binders are also used in the formulation of zeolitic materials in order to improve their mechanical performances. Nevertheless, the addition of binder in high amount may lead to an obstruction of the zeolite porosity and therefore to a decrease of the adsorption capacities of the final zeolitic material [23]. Accordingly, for the development of zeolitic materials, it is important to control binder and zeolite mass ratio in order to have both good mechanical and adsorption properties.

Previous works carried out by our team in collaboration with CNES by Lauridant *et al.* [2, 5, 8] and Rioland *et al.* [3, 4, 9] have led to the development of zeolite films, beads and pellets with good mechanical and adsorption properties. However, in the case of zeolite films, the amount of zeolite available was too small in comparison with pellets due to the low thickness of zeolitic films and for zeolite pellets, additional mechanical interfaces were needed to incorporate the pellets into the structure of satellites. That is why zeolite coatings appear to be a good alternative: i) simplicity of applying coating in the vicinity of sensitive surfaces of satellites through a spray application method, ii) large amount of zeolite available to trap Volatile Organic Compounds (VOCs). FAU-type and MFI-type zeolites turned out to be excellent candidates for this application.

The FAU-type structure possesses a three dimensional porosity and 12 membered rings windows. They consist of the connection between β -cages and hexagonal prisms which lead to the creation of large internal supercages (α -cages). Its pseudo-linear channels facilitate the diffusion of bulk hydrocarbons while its supercages act as nanoreactors adapted for hydrocarbon cracking or VOCs adsorption [24-26]. Moreover, the large pore opening of the FAU-type structure (7.4 Å) is also of great interest to trap VOCs with a kinetic diameter equal or less than 7.4 Å [3].

The MFI-structure type is characterized by a porous network formed by the interconnection of straight circular channels (5.4 Å x 5.6 Å) with sinusoidal and elliptical channels (5.1 Å x 5.4 Å). This structure is used for several environmental applications such as the removal of VOCs [2, 4, 27-29]. Depending on the silicon to aluminum molar ratio of the microporous framework, ZSM-5 and silicalite-1 are two zeolites presenting the MFI structure. The latter is the pure silica form and avoid water adsorption [29].

Even if the development of zeolite coatings remains marginal, they have already been applied by dip-coating method on aluminum substrate by using organosilane molecules as organic binders for anticorrosion [30-32] and thermal [33] applications. Silicone binder based zeolite coatings exhibited interesting mechanical, thermal and adsorption properties for thermal applications [34-36]. Inorganic binders such as metakaolin [37], bentonite [38] and colloidal silica suspensions LUDOX® [39, 40] can also be used to prepare zeolite coatings. Different types of LUDOX® were used by NASA to develop inorganic zeolite coatings for on-orbit molecular decontamination with the use of an adhesion primer to promote a good coating adherence. These inorganic coatings were developed with lower quantities of zeolite

than those involved in this study. However, the adhesion properties of inorganic binders are usually less efficient than those of coatings developed with organic binders. For the latter, the good adhesion properties are explained by the flexibility of the silicone polymer chains [36].

In this work, to achieve sufficient adhesion, cohesion, adsorption and thermal properties, the FAU-type and MFI-type zeolites previously used for the preparation of zeolite films and zeolite pellets, were separately mixed with organic and inorganic binders in water to develop hybrid zeolite coatings with high zeolite content in order to obtain high adsorption capacities of VOCs. The inorganic binder was used in the formulation of hybrid zeolite coatings in order to reduce the amount of the organic binder. Indeed, inorganic compounds are known to be stable under orbital conditions, which is not necessarily the case for organic compounds. Nevertheless, the presence of the organic binder is essential to ensure interesting adhesion properties. That is why inorganic and organic binders were used in this study to develop hybrid zeolite coatings.

The use of water as solvent is a real advantage since it does not contribute to the emission of VOCs in the atmosphere. Various methods of coating deposition are reported in the literature such as dip coating [30-33] and spray coating system [41]. The latter has been used in this work in order to have an easy-to-use and reproducible system to apply both FAU-type and MFI-type hybrid zeolite coatings on aluminum alloy substrate.

This article reports on the elaboration of high-performance green hybrid zeolite coatings as well as their characterization in relation to their adhesion and cohesion properties, textural properties and adsorption capacities of organic pollutants.

2. Experimental section

2.1. Materials

13X (FAU-type) zeolite powder with a crystal size of 2-3 μm and a Si/Al molar ratio of 1.2 was purchased from Sigma-Aldrich. Pure silica silicalite-1 (MFI-type) zeolite powder with a crystal size of 3-5 μm was provided by Zéphir Alsace company. Hereafter, zeolites are denoted as pigment in coating formulations. Organic (SILRES[®] MP 50 E) and inorganic (LUDOX[®] HS-40) binders were purchased from IMCD and Sigma-Aldrich, respectively.

The commercial product SILRES[®] MP 50 E is a methyl phenyl group containing silicone resin emulsion. For the coating formulation, the solvent recommended by the supplier is water. The product LUDOX[®] HS-40 (inorganic binder) is a suspension of colloidal silica in water.

n-Hexane (with less than 0.01 % of water, 95 % purity) was purchased from Carlo Erba. Binders and *n*-hexane were used without any further treatment.

Substrates of aluminum alloy Al 6061 (20 x 15 x 2.3 mm³) were supplied by Alfa Aesar and they were cut from plates with dimensions of 300 x 300 x 2.3 mm³.

2.2. Characterization techniques

X-Ray Diffraction (XRD)

X-Ray diffraction patterns were recorded on a PANalytical MPD X'Pert Pro diffractometer operating with Cu K α radiation ($\lambda = 0.15418$ nm) equipped with a PIXcel 1D detector (active length = $3.347^\circ 2\theta$). XRD powder patterns were collected at ambient temperature in the $3^\circ < 2\theta < 50^\circ$ range, by step of 0.013° in 2θ and with a time of 220 s by step.

X-Ray Fluorescence (XRF)

The Si/Al molar ratio of FAU-type zeolite was determined using a X-Ray fluorescence spectrometer PANalytical Zetium (4 kW).

Thermal analysis

Thermogravimetric analysis was carried out under air with a Mettler-Toledo TGA/DSC 1 equipment between room temperature and 800°C at a heating rate of $5^\circ\text{C}\cdot\text{min}^{-1}$.

Scanning Electron Microscopy (SEM) and Energy Dispersive X-Ray spectroscopy (EDX)

A scanning electron microscope JEOL JSM-7900F was used to study morphological properties of pure zeolites and hybrid zeolite coatings. Energy dispersive X-Ray mappings were obtained with Bruker XFlash detectors.

Thickness measurement

Coatings thickness measurements on non-ferrous substrates (here aluminum alloy) were carried out by using an ISOSCOPE[®] FMP10 equipped with a probe FTA3.3H purchased from Fischer.

Adhesion tests

Adhesion properties of zeolite coatings applied on aluminum alloy substrate were obtained by performing cross-cut tests with a cutting knife fitted with parallel blades supplied by TQC. A right-angle lattice pattern is cut into the coating penetrating through to the substrate. A tape is then placed over the grid and removed to evaluate qualitatively the detachment of the coating from the substrate. The resistance of the coating to separation of the substrate is evaluated using ISO 2409 classification ranging from 0 for an unaltered coating to 5 for a coating peeling off completely from the substrate (**Table 1**). In our case, adhesion is defined by the intermolecular forces responsible for the adhesion of a coating on a substrate whereas cohesion is concerning the forces responsible for interactions between zeolite particles inside a coating layer.

Nitrogen (N₂) adsorption-desorption

The textural properties of pure zeolites and zeolite coatings were determined from nitrogen adsorption-desorption isotherms performed at -196°C with a Micromeritics ASAP 2420 instrument. Before each measurement, samples were outgassed under vacuum at 150°C for 15 h to ensure that the volatile compounds adsorbed inside the porosity of the adsorbent material are driven off. The equilibrium time has been fixed at 30 s for each adsorption-desorption experiment. These experiments are used to determine the accessibility of zeolite coatings porosity compared to pure zeolites. Micropore volume was determined using the t-plot method.

Organic pollutant adsorption

The adsorption capacities of organic pollutants by zeolitic materials were studied at room temperature under *n*-hexane atmosphere inside a desiccator preliminary dried under argon flow to remove moisture. The molecule of *n*-hexane is one of the contaminants identified by NASA and CNES in satellites. It will be used as a probe molecule to determine the adsorption capacities of these zeolite coatings. Samples were previously activated under vacuum (10^{-4} mbar) at 150 °C for 15 h to remove all traces of volatile compounds from the porosity.

2.3. Preparation of green hybrid zeolite coatings

The surface of aluminum alloy substrates was first treated by physical abrasion using emery paper (with 180 μm grit) for approximately 60 s and then washed with ethanol and acetone to remove any contaminants from the surface.

In the case of the formulation of FAU-type hybrid zeolite coatings, hydrophilic 13X zeolite was saturated with water (using a desiccator containing a saturated solution of NH_4Cl to obtain a relative humidity of 80 %) to avoid the variation of the mass of zeolite 13X zeolite during weighing. The amount of water adsorbed in 13X zeolite was then determined by thermogravimetric analysis and was found to be 23 wt. %. For hydrophobic pure silica silicalite-1 (MFI) powder, an activation step was performed at 300 °C for 5 h to remove all VOCs trapped inside. Whatever the zeolite used in the formulation of coatings, the experimental protocol remains the same. Before adding SILRES[®] MP 50 E and LUDOX[®] HS-40 binders in the formulation of hybrid zeolite coatings, zeolite (pigment) was first mixed with water in an ultrasonic bath for 10 min in order to disperse zeolite in water to have a homogeneous suspension. For FAU-type and MFI-type coatings, water content was fixed respectively at 50 and 67 wt. % regarding the total weight of the suspension. Then, both binders were added to the zeolite suspension respecting a binder/pigment ratio of 40 wt. % before drying the coating. For the basic formulation, the binder part of the coating formulation consists of a mixture of SILRES[®] MP 50 E and LUDOX[®] HS-40 with 50 wt. % for each binder. The formulation was then stirred in an ultrasonic bath for 10 min to obtain a homogeneous formulation sufficiently liquid to be applied on the aluminum alloy substrate by using a spraying method. Therefore, the quantity of solvent added in the mixture is very important to control in order to obtain a satisfactory viscosity. An airbrush pistol AFC-101A from Conrad Electronics was used as sprayer for this study. Only a single layer was applied for each coating. Finally, the wet coating applied on the aluminum alloy substrate was dried at 250 °C for 30 min to obtain the final dry coating with sufficient mechanical properties and an amount of zeolite from 80 to 85 %. For the other formulations developed, only the proportion of inorganic binder to that of the organic binder has been increased to study its influence especially on adhesion and cohesion properties. The inorganic binder part has been fixed at 60, 70 and 75 wt. % with regards to the total weight of both binders before drying. All coatings are reported in **Table 2**. Zeolite coatings made only with the organic binder (FAU-MP50E and MFI-MP50E) or the inorganic binder (FAU-HS40 and MFI-HS40) were also developed to compare their mechanical and adsorption properties with those of hybrid zeolite coatings.

3. Results and discussion

3.1. Characterization of the reagents

Prior using them in the formulation of zeolite coatings, 13X zeolite and silicalite-1 zeolite powders were characterized by X-ray diffraction (XRD), scanning electron microscopy and nitrogen adsorption-desorption measurements. The XRD patterns present characteristic peaks of FAU-type and MFI-type (**Fig. 1a** and **1b**) zeolites. Scanning electron micrographs show bipyramidal and rhombohedral crystals morphologies which are characteristic of FAU-type phase (**Fig. 1c**) and MFI-type phase (**Fig. 1d**), respectively. Moreover, particles sizes are of 2-3 μm and 3-5 μm , respectively. The good crystallization rate of 13X and silicalite-1 zeolites is also confirmed by nitrogen adsorption-desorption isotherms of type I characteristics of microporous materials according to IUPAC classification [42]. Indeed, the experimental micropore volumes (0.30 $\text{cm}^3\cdot\text{g}^{-1}$ and 0.18 $\text{cm}^3\cdot\text{g}^{-1}$, respectively) are in good agreement with values of pure and well crystallized FAU-type [43, 44] and MFI-type [29, 45] zeolites reported in literature (**Fig. 1e** and **1f**).

Due to the drastic conditions encountered in orbit where temperatures can vary between -110 °C and 150 °C under high vacuum at least for external surfaces, the different constituents of the coatings and especially the organic binder SILRES[®] MP 50 E must be stable in this temperature range. Regarding zeolites (13X and silicalite-1) and the inorganic binder LUDOX[®] HS-40, these compounds are known to be stable at high temperature (> 150 °C). Consequently, the thermogravimetric analysis was only carried out on the silicone resin SILRES[®] MP 50 E (**Fig. 2**) in order to determine the maximum temperature of use. This experiment was carried out on the polymerized resin.

The TG curve of the polymerized resin (**Fig. 2**) shows that the binder can be used up to a temperature of 300 °C without decomposition. Consecutive mass losses are observed between 350 and 650 °C which correspond to the multi-step decomposition of the organic binder. They represent 60 % of the total mass of the polymerized resin. The remaining 40 % of solid corresponds to the inorganic part of the binder which consists of amorphous silica. Therefore, the drying temperature (250 °C) and the outgassing temperature (150 °C) will not affect the silicone resin.

3.2. Characterization of hybrid zeolite coatings

3.2.1. Morphological analysis

Green hybrid zeolite coatings contain around 80 wt. % of zeolite in the dry final coating compared to the amount of binders. Adding the inorganic binder LUDOX[®] HS-40 in FAU-type zeolite coatings improves the homogeneity of the coating on the aluminum alloy substrate. Indeed, a lack of homogeneity is observed when the organic binder is only present in the coating (**Fig. 3a**) whereas this phenomenon is not observed when the LUDOX[®] HS-40 is added to the coating (**Fig. 3b**). In **Fig. 4**, SEM micrographs of the surface of two hybrid zeolite coatings are reported. These micrographs show the zeolite particles on the aluminum alloy substrate and binder bridges between zeolite crystals responsible for adhesion properties of the coating on the substrate and also cohesion properties between zeolite particles inside the coating. The same observation is drawn for the other hybrid coatings and also for organic FAU-MP50E and MFI-MP50E coatings even if a lack of homogeneity at the

macroscopic scale is observed. The analysis was not performed on inorganic FAU-HS40 and MFI-HS40 coatings due to poor adhesion properties as it will be described later. The elemental distribution of Al, C, Si, Na and O atoms was also investigated on hybrid zeolite FAU-MP50E(50)-HS40(50) and MFI-MP50E(50)-HS40(50) coatings applied on aluminum alloy substrates by using EDX mappings displayed in **Fig. 5**. Both coatings exhibit a similar thickness (between 25 and 40 μm).

EDX mappings show a good complementarity between the presence of the carbon and the one of the constituent elements zeolites (see **Fig. 5**). The carbon atoms observed on the EDX mapping is due to the presence of the silicone resin SILRES[®] MP 50 E in hybrid zeolite FAU-MP50E(50)-HS40(50) and MFI-MP50E(50)-HS40(50) coatings. For the FAU-type coating, Al and Na atoms mappings have also been acquired. The same observation is drawn for the other hybrid coatings as well as organic coatings elaborated in this work.

3.2.2. Adhesion properties

Dry hybrid zeolite coatings were developed with approximately 80 to 85 wt. % of zeolite to ensure high adsorption capacities of organic pollutants and around 15 to 20 wt. % of binders in order to maintain mechanical properties and especially adhesion properties of the coating on the substrate and the cohesion properties between the zeolite particles inside the coating.

Moreover, the binder is the constituent which avoids any cracks in the coating. The adhesion properties of each coating have been characterized after the coating drying step by using the cross-cut test. According to ISO 2409 classification, an adhesion note has been attributed. The results of the cross-cut tests are summarized in **Table 3** as well as coatings composition and drying conditions. For FAU-MP50E and MFI-MP50E coatings made only with the organic binder, an adhesion note of 0 was obtained while very bad adhesion properties were observed for FAU-HS40 and MFI-HS40 coatings made only with the inorganic binder (adhesion note of 5). The presence of the organic binder SILRES[®] MP 50 E is therefore essential to maintain good adhesion properties of hybrid zeolite coatings on aluminum alloy substrates. Concerning both FAU-MP50E(50)-HS40(50) and MFI-MP50E(50)-HS40(50) coatings, the introduction of both organic and inorganic binders with a composition of 50 wt. % of each before the drying procedure promotes good adhesion properties with an adhesion note of 0 which means that the percentage of detached area from the substrate is close to 0 % (**Table 3**). Concerning FAU-MP50E-HS40 coatings where the percentage of inorganic binder was increased up to 75%, adhesion properties are less interesting with an adhesion note of 2 (**Fig. 6**). However, these results can be explained by the higher thickness of coating ranging from 60 to 100 μm which leads to a loss of cohesion properties inside the coating. Indeed, some cracks are observed after the cross-cut test. With the sprayer method, it is difficult to control the coating thickness which appears as a parameter impacting significantly the adhesion and cohesion properties. For MFI-MP50E-HS40 coatings, adhesion properties remain very interesting with an adhesion note varying from 0 to 1 (**Fig. 7**) which is explained by the low thickness of the coating (below 50 μm). Globally, the increase of the inorganic binder content (until 75 wt. %) has no influence on the adhesion and cohesion properties regardless of the hybrid zeolite coating. This observation is interesting for the intended application. Indeed, the increase of the amount of inorganic binder in the coating formulation allows to reduce the amount of organic compound and therefore the

possible VOCs emission. In summary, hybrid zeolite coatings exhibit good bonding performance on aluminum alloy substrate with a low detached area percentage. Moreover, similar adhesion properties to those of organic coatings (FAU-MP50E and MFI-MP50E) were obtained for hybrid zeolite coatings despite the amount of inorganic binder involved in each of these coatings.

In addition to good adhesion properties, zeolite coatings must have good adsorption capacities with respect to organic pollutants. Thus, it is essential to characterize the adsorption properties of the coatings for the targeted application in order to verify that the presence of binders does not lead to a partial blocking of zeolite porosity.

3.2.3. Nitrogen adsorption-desorption isotherms

The investigation of the adsorption capacities of zeolite coatings has been carried out by nitrogen adsorption-desorption measurements at $-196\text{ }^{\circ}\text{C}$ (**Fig. 8** and **9**). Inorganic FAU-HS40 and MFI-HS40 coatings were not characterized due to their low adhesion properties. These experiments were performed on powder mixtures of zeolite coatings. In order to determine the accessibility of both zeolite coatings porosity, pure 13X and silicalite-1 zeolite powders were used as references. Micropore volumes and values of porosity accessibility are summarized in **Table 4**. For FAU-type zeolite coatings, the amount of binders (20 wt. %) has no influence on the nitrogen adsorption capacities (see **Table 4**). Indeed, the corrected micropore volume of all FAU-type zeolite coatings is $0.30\text{ cm}^3\cdot\text{g}_{\text{zeolite}}^{-1}$. This value is similar to the one of pure FAU-type powder ($0.30\text{ cm}^3\cdot\text{g}^{-1}$) meaning that both binders (SILRES[®] MP 50 E and LUDOX[®] HS-40) do not block the access to the micropores when 20 wt. % of binders are used. The same behavior is observed for MFI-type zeolite coatings (15 wt. % of binders). Corrected micropore volumes (from 0.15 to $0.17\text{ cm}^3\cdot\text{g}_{\text{zeolite}}^{-1}$) are quite similar to the micropore volume of pure MFI-type powder ($0.18\text{ cm}^3\cdot\text{g}^{-1}$) which means that no zeolite pore blocking occurs when binders are mixed with it (see **Table 4**). The amount of binders added in zeolite coatings enable good adhesion, cohesion and adsorption properties. In order to simulate the adsorption capacities of organic pollutants by hybrid zeolite coatings, *n*-hexane adsorption experiments were performed on each coating.

3.2.4. Adsorption of *n*-hexane

The *n*-hexane molecule was used as probe molecule to simulate adsorption capacities of zeolite coatings with respect to an example of organic pollutant. To determine the adsorbed amount of *n*-hexane, each sample was weighted before the start of the experiment and after the samples have been placed for 24 h in the desiccator under an atmosphere of *n*-hexane at room temperature. Only 2 weighings were performed to minimize water co-adsorption for FAU-type zeolite coatings. An experiment duration of 24 h was enough to reach the saturation stage. All *n*-hexane adsorption capacities of each sample are reported in **Table 5**. The adsorbed amount of *n*-hexane in FAU-type powder obtained in this work ($180\text{ mg/g}_{\text{anhydrous zeolite}}$) is in good agreement with values reported in the literature ranging from 181 to 186 $\text{mg/g}_{\text{anhydrous zeolite}}$ [26, 46]. Adsorbed amounts of *n*-hexane between 136 and 143 $\text{mg/g}_{\text{anhydrous zeolite}}$ were measured for FAU-type hybrid zeolite coatings which are 20 to 25 % lower than the value observed for 13X powder. An adsorbed amount of $126\text{ mg/g}_{\text{anhydrous zeolite}}$ was measured for the organic FAU-MP50E coating. The lower hexane adsorption capacities could be explained by a partial co-adsorption of water which could occur during the first sample weighing. For

MFI-type zeolite samples, the *n*-hexane adsorption capacities of MFI-type hybrid zeolite coatings (from 103 to 106 mg/g_{anhydrous zeolite}) are similar to the experimental value obtained for silicalite-1 powder (110 mg/g_{anhydrous zeolite}) which is in good agreement with literature where values are ranging from 108 to 111 mg/g_{anhydrous zeolite} [29, 45, 47]. A similar result was obtained for organic MFI-MP50E coatings with an adsorbed amount of 107 mg/g_{anhydrous zeolite}. The adsorption capacities of FAU-type hybrid zeolite coatings appear to be the most interesting (**Table 5**) but for this latter a water co-adsorption phenomenon due to its hydrophilic character can occur when the material is exposed to a humid atmosphere. Despite lower *n*-hexane adsorption capacities, hydrophobic MFI-type hybrid zeolite coatings seem to be the most suitable for the adsorption of *n*-hexane in the presence of humidity. Nevertheless, hybrid zeolite coatings exhibit interesting adsorption capacities regarding an example of a linear hydrocarbon (*n*-hexane) which are promising for the targeted application. Moreover, the use of the FAU-type zeolite is also interesting due to its pore opening of 7.4 Å which gives it the ability to trap organic pollutants with a larger kinetic diameter than the one of *n*-hexane which is 4.3 Å [48].

4. Conclusion

FAU- and MFI-type green hybrid zeolite coatings were elaborated by mixing 13X or silicalite-1 zeolites with the commercial silicone resin SILRES[®] MP 50 E (organic binder) and a colloidal silica suspension in water LUDOX[®] HS-40 (inorganic binder). Both binders were combined in order to achieve sufficient adhesion and cohesion properties. Moreover, the inorganic binder was added to reduce the organic binder proportion and also to improve coating homogeneity on aluminum alloy substrates.

Cross-cut tests showed that adhesion properties are very interesting despite the small amount of binders used in hybrid zeolite coatings (20 and 15 wt. % for FAU- and MFI-type zeolite coatings, respectively).

Nevertheless, the presence of silicone resin is essential to keep interesting adhesion properties. Indeed, both zeolite coatings without organic binder were completely peeled off from the aluminum alloy substrate after the cross-cut test.

Zeolite porosity is almost 100 % accessible for hybrid zeolite coatings despite the presence of both binders and their *n*-hexane adsorption capacities are ranging from 136 to 143 mg/g_{anhydrous zeolite} and from 103 to 106 mg/g_{anhydrous zeolite} for FAU- and MFI-type hybrid zeolite coatings, respectively. These promising results show that green hybrid zeolite coatings possess high potential for on-orbit molecular decontamination.

Acknowledgements

We would like to thank Ludovic Josien, Laure Michelin and Gautier Schrodj for their assistance with the scanning electron microscopy, the X-ray diffraction and thermogravimetric analysis, respectively. Funding from the Centre National d'Etudes Spatiales (CNES), the company Zéphir Alsace and Institut Universitaire de France (IUF) is gratefully acknowledged. We would also like to thank IMCD for supplying the commercial silicone resin SILRES[®] MP 50 E.

References

- [1] J. L. Perry, NASA Tech. Memo. 108497 (1995) 4-12.
- [2] N. Lauridant, T. J. Daou, G. Arnold, M. Soulard, H. Nouali, J. Patarin & D. Faye, *Microporous Mesoporous Mater.* 152 (2012) 1-8. <https://doi.org/10.1016/j.micromeso.2011.12.012>
- [3] G. Rioland, L. Bullot, T. J. Daou, A. Simon-Masseron, G. Chaplais, D. Faye, E. Fiani & J. Patarin, *RSC Adv.* 6 (2016) 2470-2478. <https://doi.org/10.1039/c5ra23258a>
- [4] G. Rioland, T. J. Daou, D. Faye & J. Patarin, *Microporous Mesoporous Mater.* 221 (2016) 167-174. <https://doi.org/10.1016/j.micromeso.2015.09.040>
- [5] N. Lauridant, T. J. Daou, G. Arnold, H. Nouali, J. Patarin & D. Faye, *Microporous Mesoporous Mater.* 172 (2013) 36-43. <https://doi.org/10.1016/j.micromeso.2013.01.017>
- [6] J. B. Barengoltz, S. Moore, D. Soules & G. Voecks, *Jet Propul. Lab.* 94 (1994) 1-48.
- [7] H. Kirsch-Rodeschini, PhD Thesis, Haute-Alsace University (2006).
- [8] N. Lauridant, T. J. Daou, G. Arnold, J. Patarin & D. Faye, *Microporous Mesoporous Mater.* 166 (2013) 79-85. <https://doi.org/10.1016/j.micromeso.2012.04.057>
- [9] G. Rioland, H. Nouali, T. J. Daou, D. Faye & J. Patarin, *Adsorption* 23 (2017) 395-403. <https://doi.org/10.1007/s10450-017-9870-9>
- [10] M. E. Davis, 417 (2002) 813-821. <https://doi.org/10.1038/nature00785>
- [11] A. Burton, *Porous architectures*, *Nat. Mater.* 2 (2003) 438-440. <https://doi.org/10.1038/nmat937>
- [12] J. Huve, A. Ryzhikov, H. Nouali, V. Lalia, G. Augé & T. J. Daou, *RSC Adv.* 8 (2018) 29248-29273. <https://doi.org/10.1039/C8RA04775H>
- [13] I. Deroche, T. J. Daou, C. Picard & B. Coasne, *Nat. Commun.* 10 (2019) 1-10. <https://doi.org/10.1038/s41467-019-12418-9>
- [14] A. Corma, V. Gonzalez-Alfaro & A. V. Orchillès, *Appl. Catal. A* 129 (1995) 203-215. [https://doi.org/10.1016/0926-860X\(95\)00081-X](https://doi.org/10.1016/0926-860X(95)00081-X)
- [15] A. Corma, *Stud. Surf. Sci. Catal.* 49 (1989) 49-67. [https://doi.org/10.1016/S0167-2991\(08\)61708-5](https://doi.org/10.1016/S0167-2991(08)61708-5)
- [16] J. Cejka, G. Centi, J. Perez-Pariente & W. J. Roth, *Catal. Today* 179 (2012) 2-15. <https://doi.org/10.1016/j.cattod.2011.10.006>
- [17] J. Zecevic, G. Vanbutsele, K. P. de Jong & J. A. Martens, *Nature* 528 (2015) 245-248. <https://doi.org/10.1038/nature16173>
- [18] Y. S. Ok, J. E. Yang, Y. S. Zhang, S. J. Kim & D. Y. Chung, *J. Hazard. Mater.* 147 (2007) 91-96. <https://doi.org/10.1016/j.hazmat.2006.12.046>
- [19] W.-R. Lim, S. W. Kim, C.-H. Lee, E.-K. Choi, M. H. Oh, S. N. Seo, H.-J. Park & S.-Y. Hamm, *Sci. Rep.* 9 (2019) 1-10. <https://doi.org/10.1038/s41598-019-49857-9>
- [20] A. Sudagar, S. Andrejkovicova, C. Patinha, A. Velosa, A. McAdam, E. Ferreira da Silva & F. Rocha, *Appl. Clay Sci.* 152 (2018) 196-210. <https://doi.org/10.1016/j.clay.2017.11.013>
- [21] S. Workneh & A. Shukla, *J. Membr. Sci.* 309 (2008) 189-195. <https://doi.org/10.1016/j.memsci.2007.10.033>
- [22] S. Li, Z. Song, J. Bai, Q. Jiang & J. Wu, *J. Colloid Interface Sci.* 552 (2019) 27-33. <https://doi.org/10.1016/j.jcis.2019.04.094>
- [23] P. Sanchez, F. Dorado, A. Funez, V. Jimenez, M. J. Ramos & J. L. Valverde, *J. Mol. Catal. A: Chem.* 273 (2007) 109-113. <https://doi.org/10.1016/j.molcata.2007.03.076>

- [24] J. Pires, A. Carvalho, P. Veloso & M. de Carvalho, *J. Mater. Chem.* 12 (2002) 3100-3104.
<https://doi.org/10.1039/B205367E>
- [25] B. de Fonseca, J. Rossignol, I. Bezverkhyy, J. P. Bellat, D. Stuerger & P. Pribetich, *Sens. Actuators, B* 213 (2015) 558-565. <https://doi.org/10.1016/j.snb.2015.02.006>
- [26] I. Kabalan, B. Lebeau, M.-B. Fadlallah, J. Toufaily, T. Hamieh, J. P. Bellat & T. J. Daou, *J. Nanosci. Nanotechnol.* 16 (2016) 9318-9322. <https://doi.org/10.1166/jnn.2016.12884>
- [27] P. Jacobs, H. Beyer & J. Valyon, *Zeolites* 1 (1981) 161-168.
[https://doi.org/10.1016/S0144-2449\(81\)80006-1](https://doi.org/10.1016/S0144-2449(81)80006-1)
- [28] N. Floquet, J.-M. Simon, J.-P. Coulomb, J.-P. Bellat, G. Weber & G. Andre, *Microporous Mesoporous Mater.* 122 (2009) 61-71. <https://doi.org/10.1016/j.micromeso.2009.02.009>
- [29] A. F. Cosseron, T. J. Daou, L. Tzanis, H. Nouali, I. Deroche, B. Coasne & V. Tchamber, *Microporous Mesoporous Mater.* 173 (2013) 147-154. <https://doi.org/10.1016/j.micromeso.2013.02.009>
- [30] L. Calabrese, L. Bonaccorsi, A. Capri & E. Proverbio, *Prog. Org. Coat.* 77 (2014) 1341-1350.
<https://doi.org/10.1016/j.porgcoat.2014.04.025>
- [31] L. Calabrese, L. Bonaccorsi, A. Capri & E. Proverbio, *Prog. Org. Coat.* 101 (2016) 100-110.
<https://doi.org/10.1016/j.porgcoat.2016.098.001>
- [32] L. Calabrese, L. Bonaccorsi, A. Capri & E. Proverbio, *Ind. Eng. Chem. Res.* 55 (2016) 6952-6960.
<https://doi.org/10.1021/acs.iecr.6b00844>
- [33] L. Calabrese, V. Brancato, L. Bonaccorsi, A. Frazzica, A. Capri, A. Freni & E. Proverbio, *Appl. Therm. Eng.* 116 (2017) 364-371. <https://doi.org/10.1016/j.applthermaleng.2017.01.112>
- [34] P. Bendix, S. Henninger & H.-M. Henning, *Ind. Eng. Chem. Res.* 55 (2016) 4942-4947.
<https://doi.org/10.1021/acs.iecr.6b00558>
- [35] P. Bendix, G. Fuldner, M. Möllers, H. Kummer, L. Schnabel, S. Henninger & H.-M. Henning, *Appl. Therm. Eng.* 124 (2017) 83-90. <https://doi.org/10.1016/j.applthermaleng.2017.05.165>
- [36] H. Kummer, G. Fuldner & S. Henninger, *Appl. Therm. Eng.* 85 (2015) 1-8.
<https://doi.org/10.1016/j.applthermaleng.2015.03.042>
- [37] J. Temuujin, A. Minjigmaa, W. Rickard, M. Lee, I. Williams & A. van Riessen, *Appl. Clay Sci.* 46 (2009) 265-270. <https://doi.org/10.1016/j.clay.2009.08.015>
- [38] A. Frazzica, G. Fuldner, A. Sapienza, A. Freni & L. Schnabel, *Appl. Therm. Eng.* 73 (2014) 1022-1031.
<https://doi.org/10.1016/j.applthermaleng.2014.09.004>
- [39] S. Straka, W. Peters, M. Hasegawa, K. Novo-Gradac & A. Wong, *Proc. of SPIE* 7794 (2010) 1-8.
<https://doi.org/10.1117/12.864483>
- [40] N. Abraham, M. Hasegawa & S. Straka, *Proc. of SPIE* 8492 (2012) 1-11.
<https://doi.org/10.1117/12.964419>
- [41] R. Chanda, L. Wang & W. Schwieger, *Chem. Ing. Tech.* 90 (2018) 708-712.
<https://doi.org/10.1002/cite.201700150>
- [42] M. Thommes, K. Kaneko, A. V. Neimark, J. P. Oliver, F. Rodriguez-reinoso, J. Rouquerol & K. S. W. Sing, *Pure Appl. Chem.* 87 (2015) 1051-1069. <https://doi.org/10.1515/pac-2014-1117>
- [43] D. Chen, X. Hu, L. Shi, Q. Cui, H. Wang & H. Yao, *Appl. Clay Sci.* 59-60 (2012) 148-151.
<https://doi.org/10.1016/j.clay.2012.02.017>
- [44] J. Dhainaut, T. J. Daou, A. Chappaz, N. Bats, B. Harbuzaru, G. Lapisardi, H. Chaumeil, A. Defoin, L. Rouleau & J. Patarin, *Microporous Mesoporous Mater.* 174 (2013) 117-125.
<https://doi.org/10.1016/j.micromeso.2013.03.2006>

- [45] I. Kabalan, G. Riolland, H. Nouali, B. Lebeau, S. Rigolet, M.-B. Fadlallah, J. Toufaily, T. Hamieh & T. J. Daou, *RSC Adv.* 4 (2014) 37353-37358. <https://doi.org/10.1039/C4RA05567E>
- [46] U. D. Joshi, P. N. Joshi, S. S. Tamhankar, V. V. Joshi & V. P. Shiralkar, *J. Colloid Interface Sci.* 235 (2001) 135-143. <https://doi.org/10.1006/jcis.2000.7330>
- [47] K. Beschmann, S. Fuchs & L. Riekert, *Zeolites* 10 (1990) 798-801.
[https://doi.org/10.1016/0144-2449\(90\)90065-Y](https://doi.org/10.1016/0144-2449(90)90065-Y)
- [48] J.-R. Li, R. J. Kuppler & H.-C. Zhou, *Chem. Soc. Rev.* 38 (2009) 1477-1504.
<https://doi.org/10.1039/B802426J>

Tables

Table 1. ISO 2409 classification test results

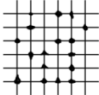
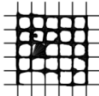
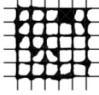
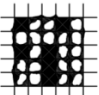
Classification ISO 2409	Description	Appearance of surface of cross-cut area from which flaking has occurred
0	The edges of the cuts are completely smooth. None of the surface of the lattice is detached.	-
1	Detachment of small flakes of the coating at the intersections of the cuts. A cross-cut area not greater than 5 % is affected.	
2	The coating has flaked along the edges and/or at the intersections of the cuts. A cross-cut area greater than 5 %, but not greater than 15 % is affected.	
3	The coating has flaked along the edges of the cuts partly or wholly in large ribbons, and/or it has flaked partly or wholly on different parts of the squares. A cross-cut area greater than 15 %, but not greater than 35 % is affected.	
4	The coating has flaked along the edges of the cuts in large ribbons, and/or some squares have detached partly or wholly. A cross-cut area greater than 35 %, but not greater than 65 % is affected.	
5	Any degree of flaking that cannot even be classified by classification 4.	-

Table 2. Composition of zeolite coatings regarding organic and inorganic binder contents and coating code

Formulation	Zeolite	SILRES® MP	LUDOX®	Coating code
		50 E (wt. %) ¹	HS-40 (wt. %) ²	
1	13X (FAU)	100	0	FAU-MP50E
2	13X (FAU)	0	100	FAU-HS40
3	13X (FAU)	50	50	FAU-MP50E(50)-HS40(50)
4	13X (FAU)	40	60	FAU-MP50E(40)-HS40(60)
5	13X (FAU)	30	70	FAU-MP50E(30)-HS40(70)
6	13X (FAU)	25	75	FAU-MP50E(25)-HS40(75)
7	Silicalite-1 (MFI)	100	0	MFI-MP50E
8	Silicalite-1 (MFI)	0	100	MFI-HS40
9	Silicalite-1 (MFI)	50	50	MFI-MP50E(50)-HS40(50)
10	Silicalite-1 (MFI)	40	60	MFI-MP50E(40)-HS40(60)
11	Silicalite-1 (MFI)	30	70	MFI-MP50E(30)-HS40(70)
12	Silicalite-1 (MFI)	25	75	MFI-MP50E(25)-HS40(75)

¹ Weight ratio of the organic binder SILRES® MP 50 E with regards to weight of both binders before drying.

² Weight ratio of the inorganic binder LUDOX® HS-40 with regards to weight of both binders before drying.

Table 3. Hybrid zeolite coatings composition, adhesion note and coating thickness

Coating code	Zeolite content (wt. %) ¹	Binder content (wt. %) ^{1, 2}	Adhesion note ³	Coating thickness (μm) ⁴
FAU-MP50E	80	20	0	10-40
FAU-HS40	83	17	5	30-50
FAU-MP50E(50)-HS40(50)	80	20	0	30-40
FAU-MP50E(40)-HS40(60)	80	20	2	70-100
FAU-MP50E(30)-HS40(70)	80	20	2	70-90
FAU-MP50E(25)-HS40(75)	80	20	2	60-80
MFI-MP50E	83	17	0	30-60
MFI-HS40	86	14	5	30-40
MFI-MP50E(50)-HS40(50)	85	15	0	25-30
MFI-MP50E(40)-HS40(60)	85	15	0	40-50
MFI-MP50E(30)-HS40(70)	85	15	1	30-50
MFI-MP50E(25)-HS40(75)	85	15	1	20-50

¹ Both zeolite and binder contents were calculated for the final dry coating.

² The binder part of the coating is made up of the mixture of silicon resin SILRES® MP 50 E and colloidal silica LUDOX® HS-40.

³ Adhesion notes according to ISO 2409 classification are ranging from 0 for an intact coating to 5 for a coating peeling off completely from the substrate.

⁴ The coating thickness was measured by using the ISOSCOPE® FMP10 equipped with the probe FTA3.3H.

Table 4. Micropore volumes and porosity accessibility of pure 13X and silicalite-1 powders and zeolite coatings (powder form) determined from nitrogen adsorption-desorption isotherms at -196 °C

Sample ¹	Micropore volume of samples (cm ³ .g ⁻¹) ¹	Corrected micropore volume (cm ³ .g _{anhydrous zeolite} ⁻¹) ²	Corrected surface area (m ² .g _{anhydrous zeolite} ⁻¹) ²	Porosity accessibility (%) ²
FAU powder	0.30	0.30	830	100
FAU-MP50E	0.24	0.30	830	100
FAU-MP50E(50)-HS40(50)	0.24	0.30	830	100
FAU-MP50E(40)-HS40(60)	0.24	0.30	830	100
FAU-MP50E(30)-HS40(70)	0.24	0.30	830	100
FAU-MP50E(25)-HS40(75)	0.24	0.30	830	100
MFI powder	0.18	0.18	420	100
MFI-MP50E	0.14	0.17	400	93
MFI-MP50E(50)-HS40(50)	0.14	0.17	400	95
MFI-MP50E(40)-HS40(60)	0.14	0.16	380	90
MFI-MP50E(30)-HS40(70)	0.14	0.17	400	93
MFI-MP50E(25)-HS40(75)	0.13	0.15	360	85

¹ Nitrogen adsorption-desorption experiments were performed on the coating mixture in powder form.

² Taking into account the amount of binders which does not adsorb N₂.

Table 5. Adsorption capacities of *n*-hexane by pure zeolites and zeolite coatings (powder form)

Sample¹	Adsorbed amount of <i>n</i>-hexane at saturation stage (mg/g_{anhydrous} zeolite)
FAU powder	180
FAU-MP50E	126
FAU-MP50E(50)-HS40(50)	136
FAU-MP50E(40)-HS40(60)	143
FAU-MP50E(30)-HS40(70)	142
FAU-MP50E(25)-HS40(75)	138
MFI powder	110
MFI-MP50E	107
MFI-MP50E(50)-HS40(50)	106
MFI-MP50E(40)-HS40(60)	103
MFI-MP50E(30)-HS40(70)	105
MFI-MP50E(25)-HS40(75)	104

¹ *n*-hexane adsorption experiments were performed on the coating mixture in powder form.

Figure captions

Figure 1. **a and b)** XRD patterns, **c and d)** scanning electron micrographs, **e and f)** nitrogen adsorption-desorption isotherms at -196 °C of 13X and silicalite-1 powders, respectively

Figure 2. TG curve of the polymerized silicone resin SILRES® MP 50 E showing the weight loss as a function of the temperature (°C)

Figure 3. FAU-MP50E coating (**a**) and FAU-MP50E(50)-HS40(50) hybrid coating (**b**)

Figure 4. SEM micrographs of hybrid zeolite coatings FAU-MP50E(50)-HS40(50) (**a and b**) and MFI-MP50E(50)-HS40(50) (**c and d**)

Figure 5. EDX mappings of Al, C, Si, Na and O atoms present in hybrid zeolite FAU-MP50E(50)-HS40(50) and MFI-MP50E(50)-HS40(50) coatings

Figure 6. Adhesion test performed on hybrid zeolite FAU-MP50E(50)-HS40(50), FAU-MP50E(40)-HS40(60), FAU-MP50E(30)-HS40(70), FAU-MP50E(25)-HS40(75) coatings, respectively (from left to right)

Figure 7. Adhesion test performed on hybrid zeolite MFI-MP50E(50)-HS40(50), MFI-MP50E(40)-HS40(60), MFI-MP50E(30)-HS40(70), MFI-MP50E(25)-HS40(75) coatings, respectively (from left to right)

Figure 8. Nitrogen adsorption-desorption isotherms of pure 13X powder and FAU-type zeolite coatings at -196 °C

Figure 9. Nitrogen adsorption-desorption isotherms of pure silicalite-1 powder (MFI) and MFI-type zeolite coatings at -196 °C

Figures

Figure 1

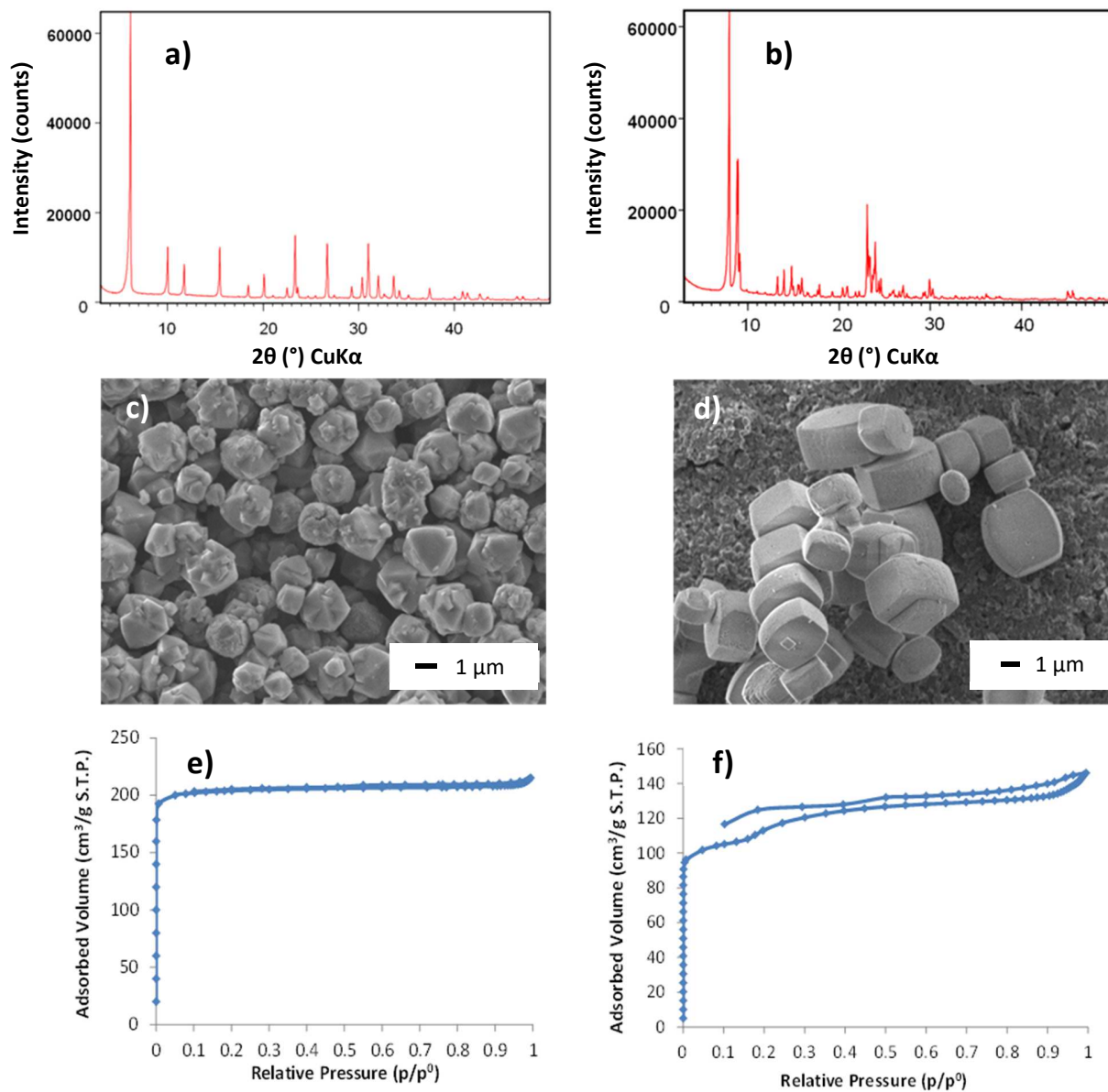


Figure 2

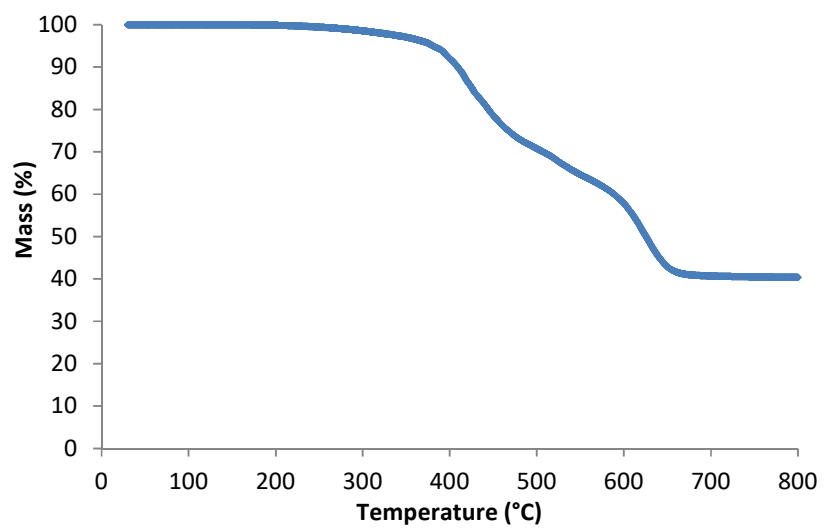


Figure 3

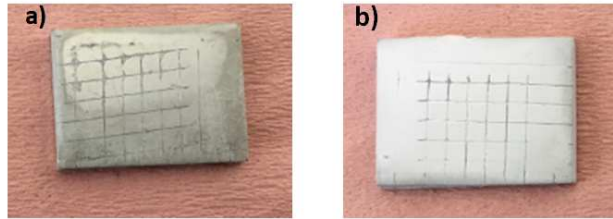


Figure 4

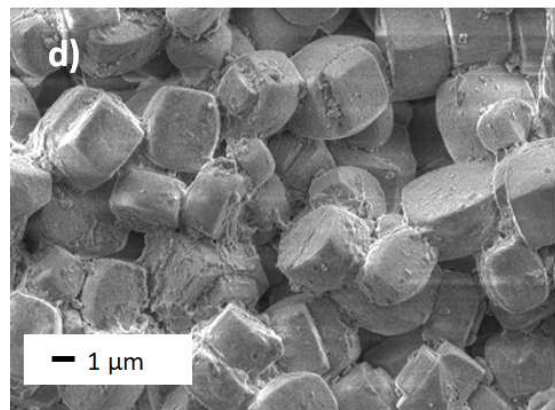
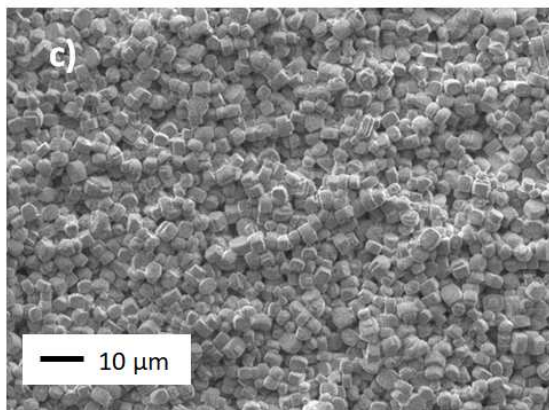
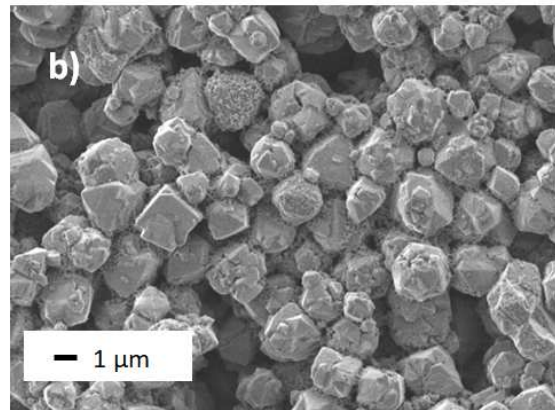
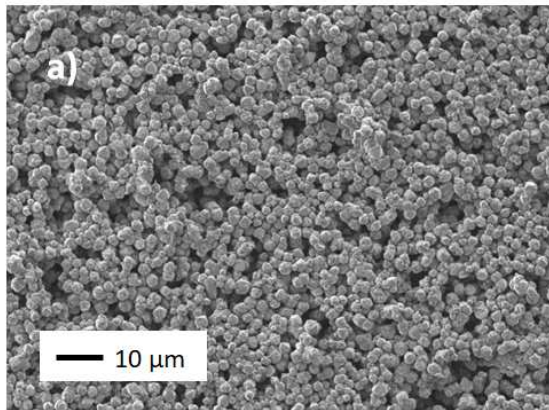


Figure 5

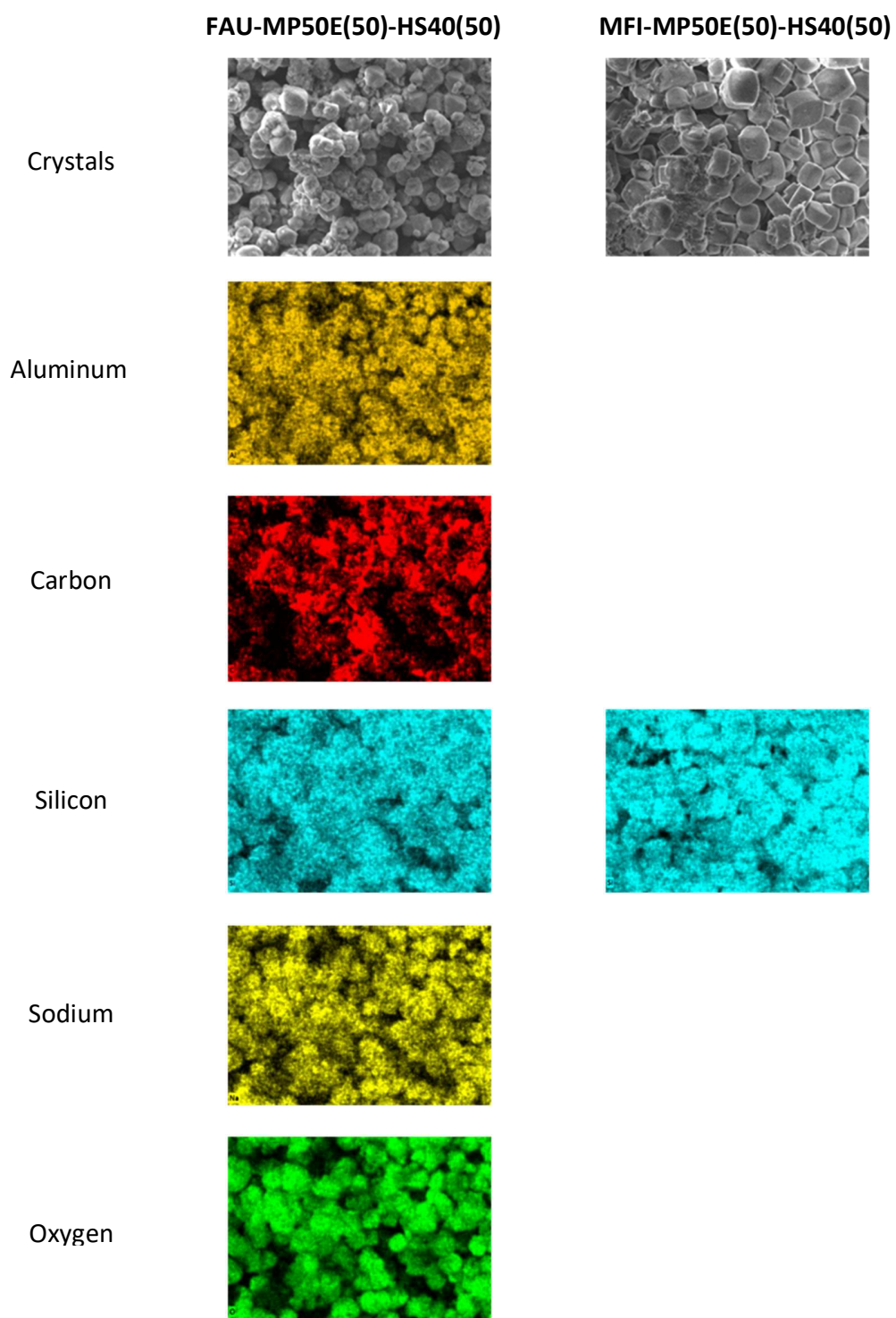


Figure 6



Figure 7

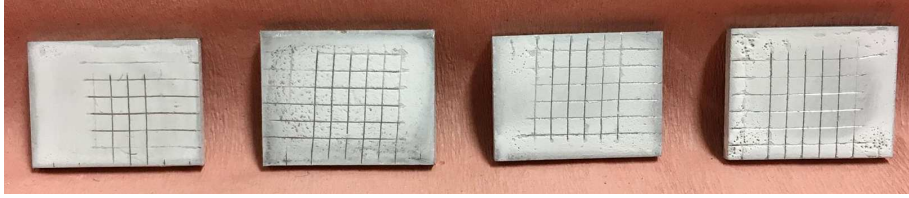


Figure 8

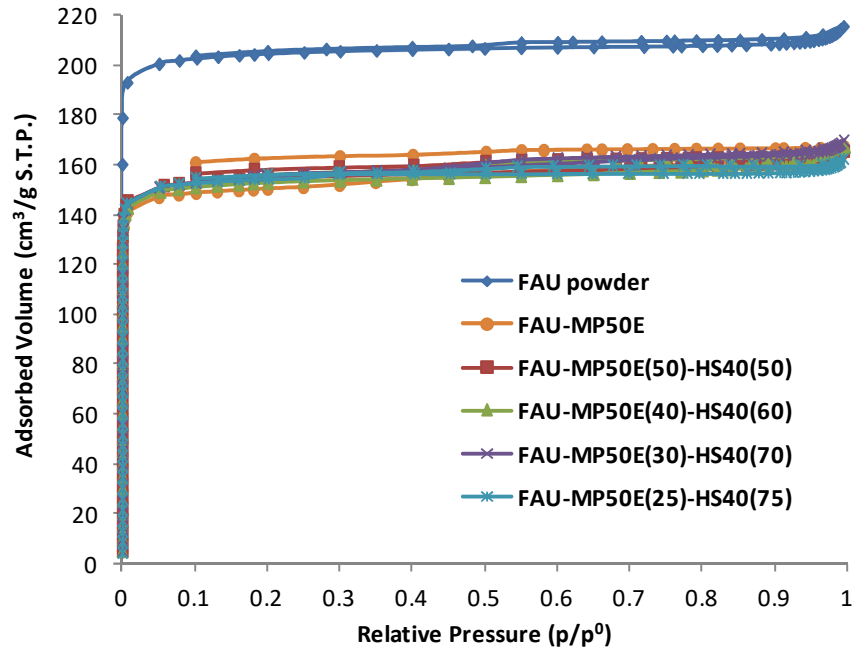
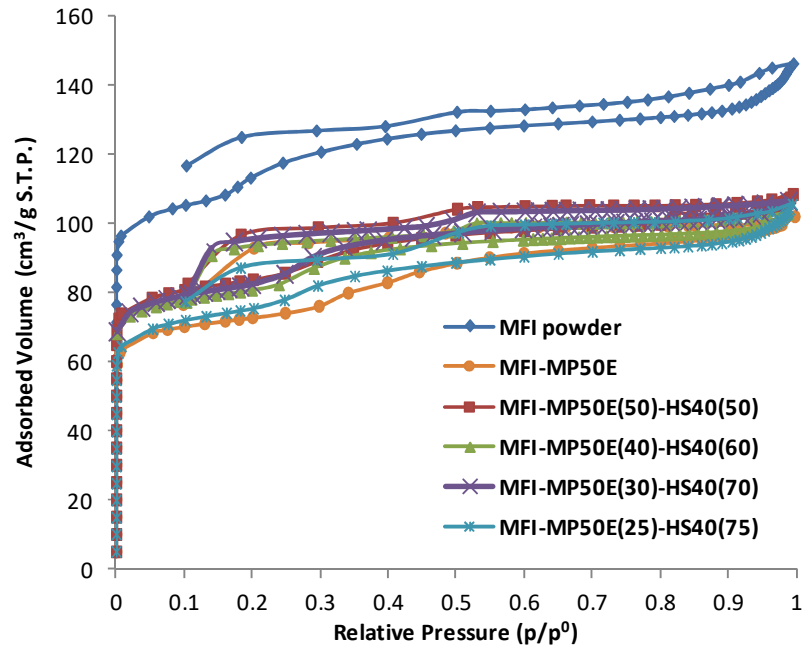
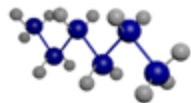
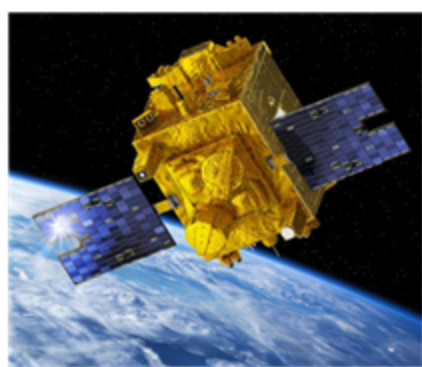
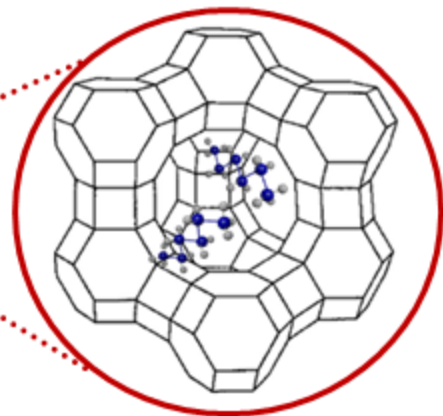
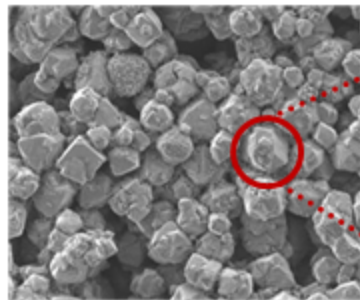


Figure 9





Outgassing of VOCs
from satellites



VOCs trapping and retention with zeolite coatings